4D reconstruction of JET DTE2 fast-ion distribution function based on synthetic data

M Rud[1], O. Hyvärinen[2], H Järleblad[3], A. Snicker[4], J Eriksson[5], Y. Dong[3], P. C. Hansen[3], M Nocente[6], B Reman[1], B. S. Schmidt[1], A Valentini[1], D Moseev[7], and M Salewski[1]

[1] *Department of Physics, Technical University of Denmark, 2800 Kgs. Lyngby, Denmark*
[2] *Department of Mathematics and Statistics, FI-00014 University of Helsinki, Finland*
[3] *Department of Applied Mathematics and Computer Science, Technical University of Denmark, 2800 Kgs. Lyngby, Denmark*
[4] *VTT Technical Research Center of Finland, Finland*
[5] *Uppsala University, 751 20 Uppsala, Sweden*
[6] *Department of Physics, University of Milano-Bicocca, 20126 Milano, Italy*
[7] *Max-Planck-Institut für Plasmaphysik, Wendelsteinstr. 1, Greifswald 17491, Germany*

Introduction In late 2021 the second deuterium-tritium campaign at the Joint European Torus (JET) was completed. Shot #99971 was designed to optimise the non-thermal fusion energy [1], and beat the previous record for the largest amount of fusion energy produced in a single shot. Here, we attempt to reconstruct the full four-dimensional (E, p, R, z) fast-ion distribution function parametrised in two spatial dimensions (R, z) and two velocity-space dimensions (E, p), with E being the energy and p the pitch of the fast ion. The tomographic reconstruction is based on synthetic data of neutron measurements calculated numerically with parameters from the shot #99971 using weight functions calculated by the OWCF code [2]. Weight functions have previously been calculated for neutron measurements in 2D velocity space [3, 4, 5] and in 3D orbit space [6, 7]. The reconstruction is obtained by solving an ill-posed inverse problem. Valuable prior information to include is that of collision physics [8, 9, 10]. Expanding the fast-ion distribution function in slowing-down expansion functions have previously been shown to improve tomographic reconstructions of the fast-ion distribution function [11, 12].

Diagnostic setup and forward problem The fast-ion diagnostic setup considered consists of three neutron detectors. First, a near-vertical sightline, KM14 [13, 14] traversing the plasma volume on the high-field side just next to the magnetic axis. Second and third, two oblique sightlines, KM15 [13, 15], and MPRu [16]. They share the line-of-sight, but the sightline of MPRu is broader than KM15. In this work, we consider synthetic data calculated from beam-target reactions as [17], $\mathbf{s} = \mathbf{s}_{\text{clean}} + \mathbf{e} = W\mathbf{f} + \mathbf{e}$. The noise covariance matrix is $(C_\mathbf{s})_{ij} = \sqrt{s_i}$ if $i = j$ and $(C_\mathbf{s})_{ij} = 0$ if $i \neq j$. Each row in the matrix W is a weight function calculated by the orbit weight computational framework [2] based on the equilibrium calculated by TRANSP [18]. The vectorised fast-ion distribution function is $\mathbf{f}$, and $\mathbf{s}_{\text{clean}}$ is the noise-free synthetic data. The data covariance matrix $C_\mathbf{s}$ is assumed to be diagonal, and the added noise $\mathbf{e}$ is Poisson distributed, since the measurements are counts of neutrons. For a large number of counts s_i, the Poisson distribution approximates the Gaussian distribution with standard deviation $\sqrt{s_i}$.

Slowing-down physics regularisation The slowing-down expansion functions are calculated numerically using the orbit-following code ASCOT [19, 20]. The expansion reads $\mathbf{f} = \sum_{i=1}^{N_{\text{sd}}} c_i \boldsymbol{\psi}_i = \Psi\mathbf{c}$, where each column in Ψ is an expansion function, and the column vector $\mathbf{c}$ contains all slowing-down coefficients c_i. Using the ASCOT code, we place 10 sources of fast ions along a radial neutral beam injector (NBI) (PINI #4 [21]) beamline and let the fast ions of each source slow down over time due to collisions to steady-state. The NBIs inject fast ions with full, one-half and one-third energy of the NBI energy. Each of the 10 sources contain all three components, such that we end up with 30 slowing-down distributions. These are the functions, which are assumed to span the space in which the true distribution lies. For the study presented in these proceedings, the true coefficients are found from a reference distribution from PINI #4 without splitting it into 10 sources. The assumed true distribution $\mathbf{f}_{\text{true}}$ is calculated using ASCOT with the equilibrium from JET shot #99971 [1]. We find the true coefficients $\mathbf{c}$ by a minimisation problem $\mathbf{c}_{\text{true}} = \min_{\mathbf{c}} ||\mathbf{f}_{\text{true}} - \Psi\mathbf{c}||_2^2$. The synthetic signal is calculated using $\mathbf{c}_{\text{true}}$. A future goal will be to add additional expansion functions, which are more likely to span the space in which the actual true experimental distribution

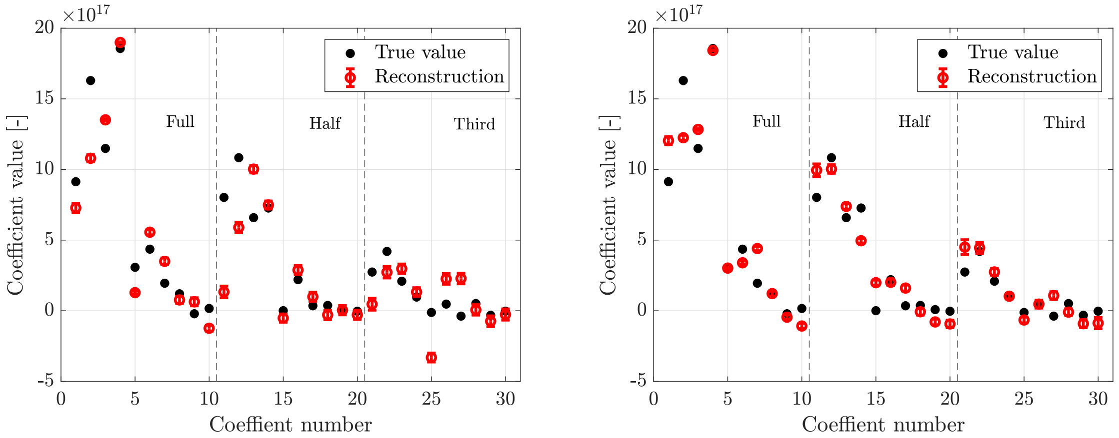

(a) Zeroth-order Tikhonov (b) First-order Tikhonov

Figure 1: Reconstruction of slowing-down coefficients using zeroth-order Tikhonov regularisation and first-order Tikhonov regularisation on the coefficients, respectively.

lives, such that experimental data can be used to reconstruct $\mathbf{f}$. Here, we use a test distribution to test that our reconstruction method is viable. Regularising the slowing-down coefficients instead of the fast-ion distribution function then reads $\bar{\mathbf{c}}_\lambda = \min_{\mathbf{c}} \left(\|\mathbf{s} - W\Psi\mathbf{c}\|^2_{C_{\mathbf{s}}^{-1}} + \lambda^2 \|L\mathbf{c}\|^2_2 \right)$, where $\bar{\mathbf{f}}_\lambda = \Psi\bar{\mathbf{c}}_\lambda$ is the optimal fast-ion distribution function reconstruction. The $C_{\mathbf{s}}^{-1}$ subscript denotes that the terms are weighted by the uncertainties. In Figure 1 we see reconstructions of the slowing-down coefficients using a zeroth-order Tikhonov and first-order Tikhonov penalisation on the coefficients respectively, including errorbars. It is evident that both techniques successfully catches the overall trend of the true values. Note that since the 10 sources are placed along the NBI beamline, the coefficient numbers are effectively labelling a radial axis.

Conclusion In conclusion, the slowing-down regularisation shows promising results in reconstructing the fast-ion distribution function using synthetic data modelled on the JET DT shot #99971. The next step is to expand this work such that the reconstruction is based on experimental data from shot #99971, to get a measure of the actual 4D fast-ion distribution function.

Acknowledgements This work has been carried out within the framework of the EUROfusion Consortium, funded by the European Union via the Euratom Research and Training Programme (Grant Agreement No 101052200 — EUROfusion). Views and opinions expressed are however those of the author(s) only and do not necessarily reflect those of the

European Union or the European Commission. Neither the European Union nor the European Commission can be held responsible for them.

References

[1] M. Maslov *et al.* Nuclear Fusion, **63**:112002, 2023.

[2] H. Järleblad *et al.* Comp. Phys. Commun., **294**:108930, 2024.

[3] M. Salewski *et al.* Nucl. Fusion, **57**:056001, 2017.

[4] M. Salewski *et al.* Fusion Science and Technology, **74**:23–36, 2018.

[5] M. Salewski *et al.* J. Instrum, **14**:C05019, 2019.

[6] H. Järleblad *et al.* Rev. Sci. Instrum., **92**:043526, 2021.

[7] H. Järleblad *et al.* Nucl. Fusion, **62**:112005, 2022.

[8] J. D. Gaffey Jr. J. Plasma Physics, **16**:149–169, 1976.

[9] W. G. F. Core. Nucl. Fusion, **33**:829, 1993.

[10] D. Moseev and M. Salewski. Phys. Plasma, **26**:020901, 2019.

[11] B. Madsen *et al.* Nucl. Fusion, **60**:066024, 2020.

[12] B. S. Schmidt *et al.* Nucl. Fusion, **63**:076016, 2023.

[13] D. Rigamonti *et al.* **64**:016016, 2024.

[14] A. Muraro *et al.* Rev. Sci. Instrum., **87**:11D833, 2016.

[15] C. Cazzaniga *et al.* Review of Scientific Instruments, **85**:043506, 2014.

[16] E. Andersson Sundén *et al.* Nucl. Instrum. Meth. Phys. Res. A, **610**:682–699, 2009.

[17] L. Stagner and W. W. Heidbrink. Phys. Plasma, **24**:092505, 2017.

[18] R. J. Hawryluk. Physics of Plasmas Close to Thermonuclear Conditions, **1**:19–46, 1980.

[19] E. Hirvijoki *et al.* Comp. Phys. Commun., **185**:1310–1321, 2014.

[20] J. Varje *et al*, 2019. arXiv:1908.02482.

[21] E. Thompson, D. Stork, H. P. L. de Esch, and the JET Teama). Phys. Fluids B: Plasma Physics, **5**(7):2468–2480, 1993.